The Journal of Neuroscience, December 15, 1996, *16*(24):7821–7831

$STEP_{61}$: A Member of a Family of Brain-Enriched PTPs Is Localized to the Endoplasmic Reticulum

Abel Bult,[1] Feisha Zhao,[1] Ronald Dirkx Jr.,[2] Ela Sharma,[3] Erika Lukacsi,[4] Michele Solimena,[2] Janice R. Naegele,[1,4] and Paul J. Lombroso[1]

[1]Child Study Center and [2]Department of Medicine, Yale University School of Medicine, New Haven, Connecticut 06520, [3]Department of Biology, Rutgers University, New Brunswick, New Jersey 08903, and [4]Program in Neuroscience and Behavior, Department of Biology, Wesleyan University, Middletown, Connecticut 06459

The STEP family of protein tyrosine phosphatases is highly enriched within the CNS. Members of this family are alternatively spliced to produce both transmembrane and cytosolic variants. This manuscript describes the distinctive intracellular distribution and enzymatic activity of the membrane-associated isoform $STEP_{61}$. Transfection experiments in fibroblasts, as well as subcellular fractionations, sucrose density gradients, immunocytochemical labeling, and electron microscopy in brain tissue, show that $STEP_{61}$ is an intrinsic membrane protein of striatal neurons and is associated with the endoplasmic reticulum. In addition, structural analysis of the novel N-terminal region of $STEP_{61}$ reveals several motifs not present in the cytosolic variant $STEP_{46}$. These include two putative transmembrane domains, two sequences rich in Pro, Glu, Asp, Ser, and Thr (PEST sequences), and two polyproline-rich domains. Like $STEP_{46}$, $STEP_{61}$ is enriched in the brain, but the recombinant protein has less enzymatic activity than $STEP_{46}$. Because $STEP_{46}$ is contained in its entirety within $STEP_{61}$ and differs only in the extended N terminus of $STEP_{61}$, this amino acid sequence is responsible for the association of $STEP_{61}$ with membrane compartments and may also regulate its enzymatic activity.

Key words: protein tyrosine phosphatase; intracellular PTP; basal ganglia; alternative splicing; SH3 domain; polyproline domain; PEST sequence; signal transduction; endoplasmic reticulum

Protein tyrosine phosphorylation plays a central role in neuronal development and function. Tyrosine phosphorylation has been implicated in axonal navigation (Winslow et al., 1995; Desai et al., 1996; Krueger et al., 1996), growth cone elongation (Maness et al., 1988), synapse formation (Qu et al., 1990; Cudmore and Gurd, 1991), cell–cell or cell–extracellular matrix interactions (Atashi et al., 1992; Doherty and Walsh, 1992), and differentiation (Girault et al., 1992; Sahin and Hockfield, 1993; Walton et al., 1993; Zhang and Longo, 1995). It is also clear that the biological effects of neurotrophic factors on neuronal survival and differentiation are partly attributable to regulating tyrosine phosphorylation (Cordon-Cardo et al., 1991; Kaplan et al., 1991; Klein et al., 1991; Schlessinger and Ullrich, 1992). These and other observations have stimulated efforts to identify novel neuronal protein tyrosine phosphatases (PTPs) and protein tyrosine kinases (PTKs) and to characterize their functions within the CNS (for review, see Walton and Dixon, 1993; Naegele and Lombroso, 1994; Bult et al., 1995).

The PTPs are classified on the basis of their structural organization and are broadly divided into receptor-like or intracellular PTPs (for review, see Fischer et al., 1991; Tonks et al., 1991; Charbonneau and Tonks, 1992). The STEP family comprises intracellular PTPs enriched within the basal ganglia and related structures (Lombroso et al., 1991, 1993; Boulanger et al., 1995; Sharma et al., 1995). Immunocytochemical and biochemical studies have demonstrated that the STEP family of polypeptides includes a group of lower molecular weight (MW) proteins enriched in cytoplasm and a group of higher MW proteins associated with particulate fractions (Lombroso et al., 1993; Boulanger et al., 1995). We reported previously the isolation of several STEP-related cDNAs (Li et al., 1995; Sharma et al., 1995). The present study was undertaken to better understand the structural and functional characteristics of one of these clones, $STEP_{61}$.

A major finding of this work is that $STEP_{61}$ is targeted to the endoplasmic reticulum (ER) of neurons. Outside of the nervous system, PTPs have been identified that are targeted to the cytoskeleton (Gu et al., 1991; Yang and Tonks, 1991; Sawada et al., 1994), the perinuclear region (Cool et al., 1990; Faure and Posner, 1993), the plasma membrane of neurosecretory granules (Solimena et al., 1996), and the nucleus (McLaughlin and Dixon, 1993; Flores et al., 1994). To date, the subcellular localization to the ER of two intracellular PTPs has been reported (Frangioni et al., 1992; Woodford-Thomas et al., 1992; Lorenzen et al., 1995). The present work is notable in that it is the first demonstration of such a localization within the CNS and includes electron microscopic, biochemical, and immunocytochemical data.

MATERIALS AND METHODS

Reagents. All reagents and chemicals were obtained from Sigma (St. Louis, MO) unless otherwise indicated.

Sequence analysis. Sequence analysis of $STEP_{61}$ was performed using

Received July 22, 1996; revised Sept. 16, 1996; accepted Sept. 24, 1996.

This work was supported by the National Alliance for Research on Schizophrenia and Depression, NATO, and National Institutes of Health Grants P0149351, MH52711, NS35989 (P.J.L.), MH18268 (A.B.), and EY09749 (J.R.N.), and by a Juvenile Diabetes Foundation Career Development Award (M.S.). The sequence reported in this article was submitted to GenBank under accession number U28217. A.B. and F.Z. contributed equally to this work. We thank P. DeCamilli, R. Jahn, J. Leckman, M. Ogren, and F. Vaccarino for critical review of this manuscript; and Reinhard Jahn and Ari Helenius, Yale University School of Medicine, for antibodies against synaptophysin and calnexin.

Correspondence should be addressed to Dr. Paul Lombroso, Child Study Center, 230 South Frontage Road, New Haven, CT 06520-0900.

Dr Bult's present address: Michigan State University, Department of Psychology, Psychology Research Building, East Lansing, MI 48824.

the MacVector sequence analysis software (Eastman Kodak, New Haven, CT), and homologies with other sequences were determined using the GCG software package (University of Wisconsin). To determine PEST sequence scores, the PEST-FIND program (Rogers et al., 1986) was obtained through the generosity of Dr. M. Rechsteiner (University of Utah).

Northern analysis. Poly(A^+) RNA was obtained from different mouse tissues, and ~2 μg was electrophoresed on a 1.2% agarose–formaldehyde gel, transferred to nylon membrane, and fixed by UV irradiation (blot obtained from Clontech). A $STEP_{61}$-specific probe was generated using PCR amplification and was ^{32}P-randomly primed. Primers used to generate this 327 bp probe were 5′-AGCTCG GATCCA CTAGTA ACGGCC-3′ (sense oligomer, nucleotides 1–24) and 5′-ACATTT CTT-TGT CGACGT CCACCG-3′ (antisense oligomer, nucleotides 304–327). Hybridization was performed under stringent conditions as described (Lombroso et al., 1991). Films were exposed overnight at −80°C with intensifier screens.

Filters were stripped and reprobed using a cDNA for a 28 S ribosomal protein to compare amounts of RNA loaded per lane. Equivalent amounts of mRNA were loaded in all lanes, except for a slight underloading of spleen. However, prolonged exposure (1 week) did not reveal STEP mRNA transcripts in this tissue. This is consistent with previous Northern analyses using the full-length $STEP_{46}$ cDNA in which no STEP transcripts were detected in spleen after 2 week exposures (Lombroso et al., 1991).

Immunoblotting. Ten percent SDS–polyacrylamide gels were used according to the method of Laemmli (1970) and Towbin et al. (1979). Adult female Long Evans rats were killed and decapitated and their brains rapidly removed. For total brain homogenates, CNS tissue was homogenized with a Teflon homogenizer in glass at a speed of 2000 rpm for 10 strokes in homogenization buffer (0.32 M sucrose, 4 mM HEPES, pH 7.3, 1 mM phenylmethylsulfonyl fluoride (PMSF), 10 mM EDTA, 1 mM benzamidine, 0.2 mg/ml aprotinin), and protein concentrations were determined using the method of Bradford (1976). Protein samples were aliquoted and stored at −80°C until further processed.

Antibodies included a monoclonal antibody generated against STEP isoforms (23E5), diluted 1:2000 (Boulanger et al., 1995); a rabbit polyclonal antibody generated against the synaptic vesicle protein synaptophysin (p38), diluted 1:250 (kindly provided by Dr. R. Jahn, Yale University School of Medicine); and a rabbit polyclonal antibody generated against the ER protein α-calnexin, diluted 1:250 (kindly provided by Dr. A. Helenius, Yale University School of Medicine). The specificity of the STEP monoclonal antibody (23E5) has been established previously by the loss of immunoreactivity on both Western blots and immunohistochemistry after preabsorption with STEP fusion protein or the peptide used as the immunogen (Boulanger et al., 1995).

Brain cell fractionation was adapted from Huttner et al. (1983) to obtain P1, P2, P3, S3, LP1, LP2, and LS2. Continuous sucrose gradients were performed following the protocol of Walch-Solimena et al. (1993). In brief, P3 and LP2 pellets were resuspended in 0.32 M sucrose buffer and layered on top of a continuous sucrose gradient (0.4–2 M). Gradients were ultracentrifuged for 5 hr at 65,000 × *g* at 4°C. Aliquots were removed and analyzed for refractive index calculation for verification of the density gradient. Samples were stored at −80°C until further analysis.

To determine the nature of the association of $STEP_{61}$ with membrane fractions, P3 pellets were washed in different buffers and ultracentrifuged, and the resulting pellet and supernatants were analyzed by immunoblotting. Approximately 1 mg of the P3 pellet was resuspended in 0.32 M sucrose, 10 mM HEPES and either 1 M NaCl, 0.1 M Na_2CO_3, pH 11.5, 2% Triton X-100, or 1% SDS was added to each tube. Samples were then incubated on ice for 30 min and ultracentrifuged at 200,000 × *g* for 1 hr (Fujiki et al., 1982). Equivalent amounts of supernatant and pellets were analyzed for $STEP_{61}$ by immunoblot.

Deglycosylation. Deglycosylation of brain membrane fractions were essentially as described previously (Naegele and Barnstable, 1991). P3 and LP2 fractions were diluted to a final concentration of 1 mg/ml in incubation buffer (100 mM potassium phosphate, pH 7.9, 25 mM EDTA, 1% Triton X-100, 0.2% SDS, 1% β-mercaptoethanol, 0.5 mM PMSF), boiled for 3 min, and cooled on ice. After the addition of 25 U of N-glycosidase F (Boehringer Mannheim, Indianapolis, IN), the samples were incubated overnight at 37°C with shaking. Control samples were treated identically except that the enzyme was omitted. Samples (50 μg) were loaded onto 10% SDS–polyacrylamide gels, transferred to nitrocellulose, and immunoblotted with anti-STEP antibody (23E5) or anti-synaptophysin antibodies.

Transfections. The open reading frames (ORFs) of $STEP_{61}$ and $STEP_{46}$ were amplified using PCR with clone-specific primers containing an *Xba*I restriction site. Amplified fragments were placed in both sense and antisense orientation at the unique *Xba*I site of the eukaryotic expression vector pRc/CMV (In vitrogen, San Diego, CA) and checked for proper orientation by restriction enzyme digestions. DNA was purified by two cesium chloride ultracentrifugations before use in transient transfections of Chinese Hamster Ovary (CHO) cells using 10 μg of plasmid DNA with 30 μl of lipofectin (1 mg/ml, Life Technologies, Grand Island, NY) as described previously (Solimena et al., 1993).

Immunohistochemistry. A $STEP_{61}$-specific antibody was generated by immunizing rabbits with a 20 amino acid synthetic peptide present in $STEP_{61}$ and absent in $STEP_{46}$ (amino acids 36–55) (Fig. 1*A*). Crude antiserum from rabbit "Nod" was affinity-purified as follows: antiserum was diluted twofold in 0.1 M Na_2CO_3, pH 7.2 and centrifuged at 10,000 × *g* for 20 min, and total IgG was isolated on a G-protein column (BioRad, Melville, NY). The eluant was subsequently affinity-purified on a $STEP_{61}$ fusion protein column and dialyzed extensively before use. CHO cells were transiently transfected with either $STEP_{61}$ or $STEP_{46}$ cDNA and were fixed and processed for immunocytochemistry as described previously (Cameron et al., 1991). For immunohistochemical analyses, dilutions for Nod ranged from 1:10 to 1:400, and for the monoclonal antibody 23E5, which recognizes all isoforms isolated to date, the dilution was 1:80. Secondary antibodies were rhodamine-conjugated goat anti-rabbit or anti-mouse IgG at 1:50 dilution. Because the Nod antiserum does not stain STEP isoforms in Western blot experiments, the monoclonal was used for those experiments (Boulanger et al., 1995).

A marker for the ER, protein disulfide isomerase (PDI) (mouse monoclonal anti-PDI, clone 1D3, StressGen, Sidney, Canada) was colocalized with $STEP_{61}$ by two-color immunofluorescent staining in two adult rats. The CNS was fixed by transcardiac perfusion, and staining was performed as described previously, with slight modifications (Dunn et al., 1995; Raghunathan et al., 1996). Sections were incubated in a cocktail of Nod (1:200) and anti-PDI (1:600) overnight at RT. After extensive washing, sections were labeled with a cocktail of secondary antibodies; PDI immunoreactivity was detected with a horse anti-mouse IgG-Texas Red (1:500, Vector, Burlingame, CA), and $STEP_{61}$ was detected with a biotinylated goat anti-rabbit IgG (1:300, Vector), followed by streptavidin-FITC (1:1000, Vector). After extensive washes, sections were coverslipped in Vectashield (Vector) and photographed on a Zeiss Axiophot fluorescence photomicroscope.

Immunoelectron microscopy. Deeply anesthetized Long Evans rats were perfused with 0.1 M sodium phosphate buffer, pH 7.4, containing 0.1 U/ml sodium heparin, followed by perfusion with ~250 ml of a fixative containing 4% paraformaldehyde and 0.2% glutaraldehyde in 0.1 M phosphate buffer, pH 7.4. The brains were left in the skull for 2 hr at 4°C, removed, blocked, and post-fixed in the perfusion solution for 4 hr (Naegele et al., 1988). Vibratome sections (100 μm thick) were cut in coronal plane and collected in cold 0.1 M phosphate buffer. For EM embedding, sections were post-fixed in 1% osmium tetroxide for 30 min on ice. Sections were dehydrated in ethanol and propylene oxide (EM Sciences, Gibbstown, NJ). Tissue strips of striatum were embedded in LR White (Ted Pella, Redding, CA) and cured for 48 hr at 56°C in a vacuum oven. Semithin sections (1 μm thick) were cut with an LKB ultramicrotome and stained with 1% toluidine blue and basic fuchsin. Ultrathin sections (90 nm) were cut with a diamond knife and collected on 200 mesh Formvar-coated nickel grids (EM Sciences).

The procedure for EM immunolabeling is essentially as described by Griffiths et al. (1984). Ultrathin sections were incubated on the grids in a blocking solution of 1% BSA (type V, Sigma) in PBS, then in Nod sera (1:10) or anti-synaptophysin (1:50). After extensive washing, primary antibodies were detected by incubating grids in A-protein–gold probes (15 nm, Drs. Posthuma and Slot, Utrecht University, The Netherlands) diluted 1:45 in 0.1% BSA in PBS for 1 hr at room temperature. Control sections were incubated in protein A-gold alone or in Nod antibody that was preabsorbed with 20 μg of $STEP_{61}$ peptide. All incubations were performed overnight at 4°C. Stained grids were washed in PBS, stabilized in 1% glutaraldehyde, washed, then stained with 2.5% uranyl acetate for 10 min and 2% lead citrate for 5 min. Sections were examined in a Zeiss transmission electron microscope with an acceleration voltage of 80 kV.

Phosphatase assays. Construction of glutathione S-transferase fusion proteins in the bacterial expression vector pGEX-2T (Smith and Johnson, 1988) was performed as described previously (Lombroso et al., 1993). The entire ORF $STEP_{61}$ was used for these constructs. Controls for these experiments included a previously constructed $STEP_{46}$-GST and GST-

A

```
Met Cys Cys Ser Glu Arg Leu Leu Gly Leu Pro Gln Pro Val Glu Met Glu Ala Pro Asp   20
Glu Ala Glu Gly Leu Pro Ser Lys Gln[Lys Glu Met Pro Pro Pro Pro Pro Pro Ser Pro   40
Pro Ser Glu Pro Ala Gln Lys]Leu Pro Pro Gln Gly Ala Gly Ser His Ser Leu Thr Val   60
Arg Ser Ser Leu Cys Leu Phe Ala Ala Ser Gln Phe Leu Leu Ala Cys Gly Val Leu Trp   80
Leu Ser Gly His Gly His Ser Trp Leu Gln Asn Thr Thr Asp Leu Ile Ser Ser Ser Leu  100
Thr Val Leu Asn His Leu Gly Pro Val Ala Trp Leu Gly Ser Gly Thr Trp Gly Ile Pro  120
Ser Leu Leu Leu Val Ser Leu Thr Val Ser Leu Val Ile Val Thr Thr Leu Val Trp His  140
Leu Leu[Lys Ala Pro Pro Glu Pro Pro Ala Pro Leu Pro Pro Glu Asp Arg]Arg Gln Ser  160
Val Ser Arg Gln Pro Ser Phe Thr Tyr Ser Glu Trp|Met Glu Glu Lys Val Glu Asp Asp  180
Phe Leu Asp Leu Asp Ala Val Pro Glu Thr Pro Val Phe Asp Cys Val Met Asp Ile Lys  200
Pro Glu Thr Asp Pro Ala Ser Leu Thr Val Lys Ser Met Gly Leu Gln Glu Arg Arg Gly  220
Ser Asn Val Ser Leu Thr Leu Asp Met Cys Thr Pro Gly Cys Asn Glu Glu Gly Phe Gly  240
Tyr Leu Val Ser Pro Arg Glu Glu Ser Ala His Glu Tyr Leu Leu Ser Ala Ser Arg Val  260
Leu Arg Ala Glu Glu Leu His Glu Lys Ala Leu Asp Pro Phe Leu Leu Gln Ala Glu Phe  280
Phe Glu Ile Pro Met Asn Phe Val Asp Pro Lys Glu Tyr Asp Ile Pro Gly Leu Val Arg  300
Lys Asn Arg Tyr Lys Thr Ile Leu Pro Asn Pro His Ser Arg Val Arg Leu Thr Ser Pro  320
Asp Pro Glu Asp Pro Leu Ser Ser Tyr Ile Asn Ala Asn Tyr Ile Arg Gly Tyr Ser Gly  340
Glu Glu Lys Val Tyr Ile Ala Thr Gln Gly Pro Ile Val Ser Thr Val Ala Asp Phe Trp  360
Arg Met Val Trp Gln Glu Arg Thr Pro Ile Ile Val Met Ile Thr Asn Ile Glu Glu Met  380
Asn Glu Lys Cys Thr Glu Tyr Trp Pro Glu Glu Gln Val Val His Asp Gly Val Glu Ile  400
Thr Val Gln Lys Val Ile His Thr Glu Asp Tyr Arg Leu Arg Leu Ile Ser Leu Arg Arg  420
Gly Thr Glu Glu Arg Ser Leu Lys His Tyr Trp Phe Thr Ser Trp Pro Asp Gln Lys Thr  440
Pro Asp Arg Ala Pro Pro Leu Leu His Leu Val Arg Glu Val Glu Glu Ala Ala Gln Gln  460
Glu Gly Pro His Cys Ser Pro Ile Ile Val His Cys Ser Ala Gly Ile Gly Arg Thr Gly  480
Cys Phe Ile Ala Thr Ser Ile Cys Cys Gln Gln Leu Arg Arg Glu Gly Val Val Asp Ile  500
Leu Lys Thr Thr Cys Gln Leu Arg Gln Asp Arg Gly Gly Met Ile Gln Thr Cys Glu Gln  520
```

B

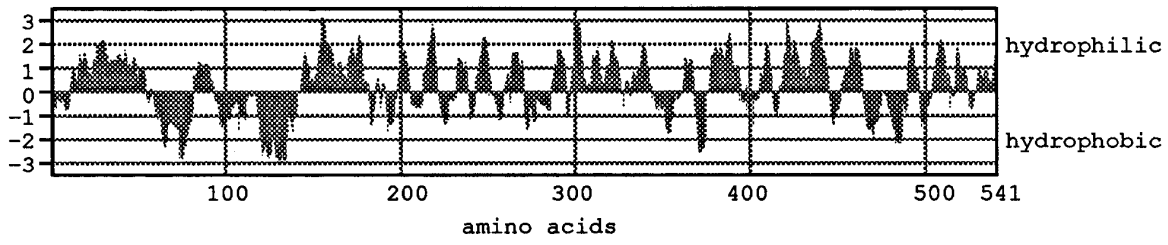

C

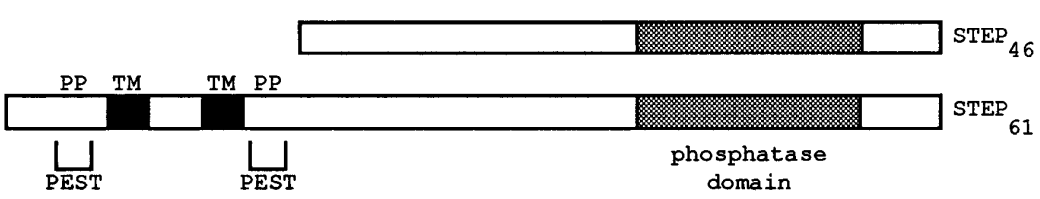

Figure 1. $STEP_{61}$ encodes a PTP with two transmembrane, two PEST sequences, and two potential SH3 binding sites. *A*, The two hydrophobic domains are indicated by the *double underline*, and the two polyproline-rich domains are indicated by a *single underline*. Two PEST sequences are enclosed in *brackets*, and the phosphatase domain is shown in *bold*. Five conservative amino acid changes from the original rat $STEP_{46}$ sequence are indicated by *asterisks* and reflect the expected variations of sequence between mouse and rat. $STEP_{46}$ sequence begins at methionine residue 173 (indicated by a *vertical bar*). *B*, Hydrophilicity analysis of the $STEP_{61}$-predicted amino acid sequence indicates two stretches of hydrophobic amino acids of 20 and 23 amino acids are present at the N terminus. The plot was obtained using the MacVector sequence analysis software and a Kyte–Doolittle algorithm with a window of seven amino acids. *C*, Schematic representation of $STEP_{61}$ and comparison with the cytosolic STEP variant $STEP_{46}$. The transmembrane domains (*TM*), PEST sequences, and polyproline domains (*PP*) are shown.

alone fusion protein (Lombroso et al., 1993). Transformed cells were induced with isopropyl-β-D-thiogalactopyranoside (IPTG), and fusion proteins were affinity-purified using glutathione-agarose beads (Sigma). For some experiments, digestion of recombinant fusion proteins was performed by the addition of excess thrombin (2 μg) to 150 μl of buffer (50 mM Tris, pH 7.5, 150 mM NaCl, 2.5 mM $CaCl_2$, 0.1% 2-mercaptoethanol) at room temperature for 1 hr with shaking. GST and uncut fusion protein were removed by affinity purification against gluta-

thione–agarose beads. Enzymatic assays were conducted in the presence of 1% Triton X-100 and used *para*nitrophenyl phosphate (*p*NPP) as substrate. Assays were performed in imidazole buffer, pH 6.2, with 1.9 mM *p*NPP for 30 min at 30°C, and the reactions were terminated by adding 900 μl of 0.2N NaOH. The production of *para*nitrophenolate ion was expressed as a concentration using a molar extinction coefficient of 1.78×10^4 M^{-1} cm^{-1} at 410 nm.

RESULTS

Structural analysis of $STEP_{61}$

The full-length cDNA clone encodes a peptide of 541 amino acids with a predicted MW of 61 kDa (Fig. 1*A*). A single PTP catalytic sequence VHCSAGIGRTG (residues 470–480) is present and conforms to the consensus sequence (I/V)HCXAGXXR(S/T)G found in members of this family (Charbonneau et al., 1989; Fischer et al., 1991). $STEP_{61}$ contains the entire $STEP_{46}$ amino acid sequence at its COOH end and 172 novel amino acids at its N terminus. Five amino acids differ between the shared sequences. The original $STEP_{46}$ clone was isolated from a rat brain cDNA library, and these changes represent conservative amino acid changes found among related species.

The 172 amino acids at the N terminus of $STEP_{61}$ contain several motifs that may have functional significance. First, there are two potential transmembrane domains of 20 and 23 hydrophobic amino acids, respectively (Fig. 1*A*,*B*). Second, two PEST sequences are present (*A*). These sequences are defined as stretches of amino acids that begin and end with a positively charged residue (H, K, or R) and contain at least eight internal residues. The internal sequences are enriched for P, E, D, S, and T and are identified by calculating a PEST score of between −50 and +35. To qualify as a PEST sequence, the PEST score value must be >-5.0. When the stretch lacks E/D or S/T, then its PEST score must be >0 (Wang et al., 1989). The two PEST sequences of $STEP_{61}$ have highly positive scores of 18 and 16, respectively. Third, two polyproline-rich domains are present and match the consensus sequence for the binding site for proteins containing SH3 domains (Fig. 1*A*) (Ren et al., 1993; Yu et al., 1994; Cohen et al., 1995). Finally, a putative site for N-glycosylation is present at the asparagine at amino acid position 91.

Northern analyses

Northern analyses were performed on various mouse organs to determine the expression patterns of $STEP_{61}$ transcripts (Fig. 2). An ~3 kb transcript is detected in brain using a $STEP_{61}$-specific probe. These results are similar to what has been found with all previously identified members of the STEP family, which have been detected in brain only and not in the peripheral tissues tested (Lombroso et al., 1991, 1993; Sharma et al., 1995; Raghunathan et al., 1996). In the present study, we also probed against mRNA obtained from skeletal muscle and testes. A transcript of ~3 kb is present in testes and a smaller transcript (2.8 kb) in skeletal muscle. It is not yet known whether these additional mRNA transcripts encode STEP-related peptides or are the result of cross-hybridization with unrelated transcripts. Prolonged exposure (1 week) did not reveal hybridization signals from the other tissues tested (data not shown). The similarity in size between the cDNA (3158 bp) and the signal seen on Northern analysis suggests that the full-length, or near full-length, cDNA was obtained.

Biochemical analyses

The distribution of $STEP_{61}$ in brain was determined by immunoblotting after subcellular fractionations. As shown in Figure 3*A*, a group of STEP-immunoreactive bands with apparent MWs between 60 and 66 kDa were enriched in particulate fractions (P3 and LP2) and were not detected in soluble fractions (S3 and LS2). P3 and LP2 fractions were enriched with small organelles and membranes from either neuronal cell bodies or synaptosomes, respectively. These results confirm earlier findings showing enrichment of higher MW STEP-immunoreactive polypeptides in particulate fractions, whereas lower MW STEP immunoreactive proteins are detected in soluble as well as in particulate fractions (Fig. 3*A*) (Boulanger et al., 1995). As expected, the membrane marker of synaptic vesicles, synaptophysin (p38) (Jahn et al., 1985), was detected in particulate fractions only.

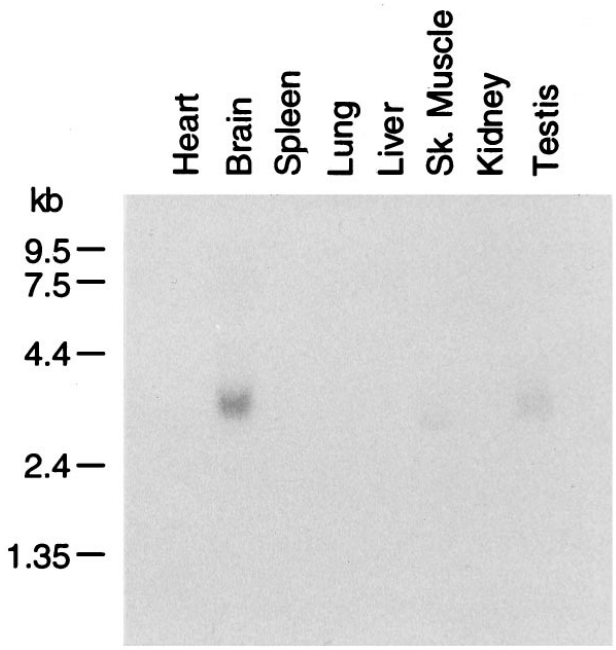

Figure 2. $STEP_{61}$ mRNA is enriched in the CNS. Poly(A^+)-selected mRNA (2 μg) from the indicated mouse organs was loaded onto a denaturing gel, electrophoresed, and transferred to nylon membrane. A $STEP_{61}$-specific probe was generated by PCR and randomly primed with ^{32}P. After 18 hr of hybridization, the blot was washed and exposed with intensifying screens overnight at −80°C.

To establish the relationship between the higher MW STEP-immunoreactive bands and the product of the $STEP_{61}$ cDNA, we compared the mobility of the recombinant $STEP_{61}$ protein with endogenous STEP isoforms. For this purpose, the $STEP_{61}$-GST fusion protein was digested with thrombin before immunoblotting (Fig. 3*B*). The recombinant protein had a very similar mobility to the higher MW membrane-enriched isoforms present in P3 (Fig. 3*B*, *lane 2*), suggesting that the isolated cDNA encodes one of these higher MW STEP variants. However, this experiment did not allow us to identify the specific polypeptide that corresponds to $STEP_{61}$.

Next, we assessed whether varying levels of glycosylation might generate the multiple STEP-immunoreactive bands observed in particulate fractions. N-glycosidase F selectively removes asparagine-linked oligosaccharides from glycoproteins and should alter the electrophoretic mobility of $STEP_{61}$ if it were glycosylated. Treated samples were separated by SDS-PAGE, and immunoreactivity for $STEP_{61}$ and the glycoprotein synaptophysin was detected on Western blots (Fig. 3*C*). As reported previously (Rehm et al., 1986), digesting membrane fractions with

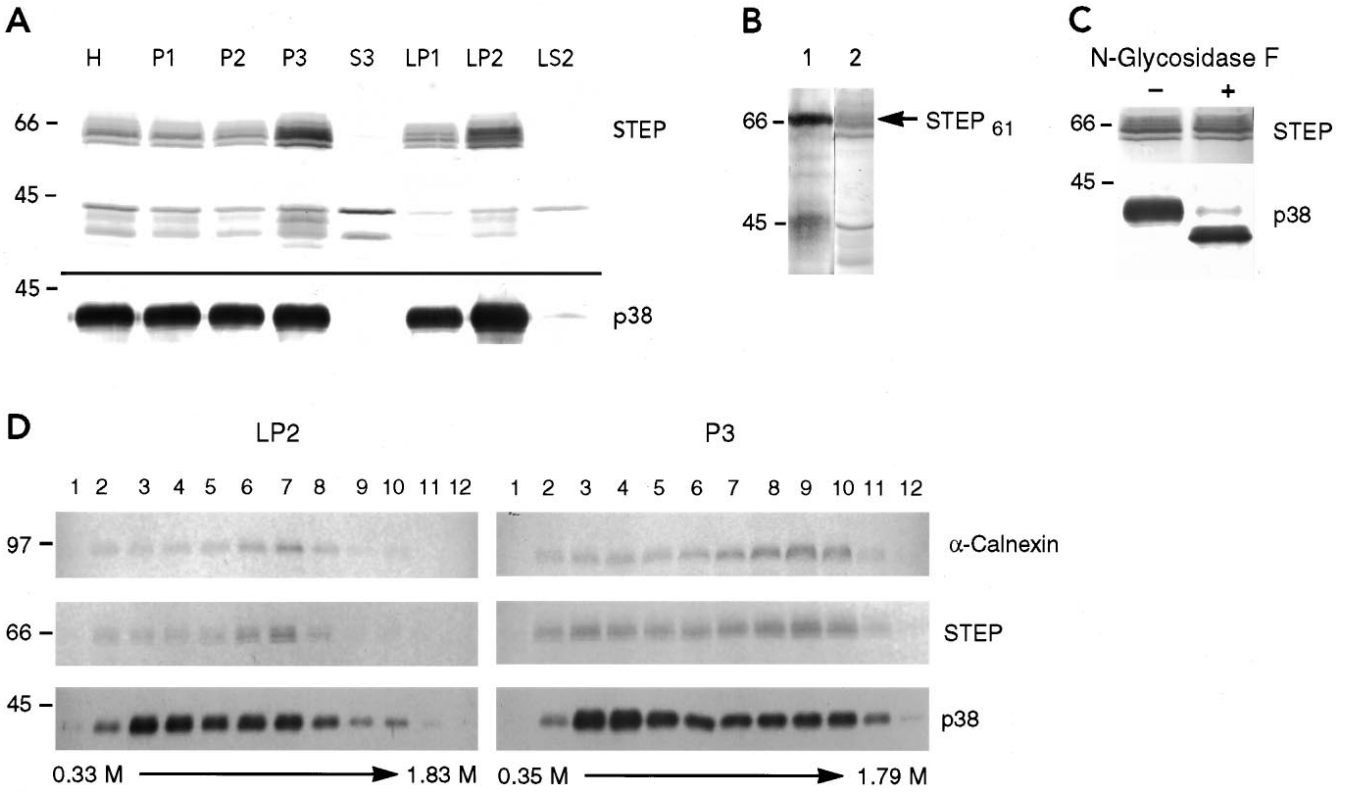

Figure 3. $STEP_{61}$ in brain: biochemical analysis. *A*, Immunoblots of subcellular fractionation of rat brain. Equivalent amounts of protein from each fraction (50 μg) were subjected to SDS-PAGE, transferred to nitrocellulose, and probed with the $STEP_{61}$ monoclonal antibody 23E5 and with a polyclonal antibody against synaptophysin (p38). *H*, Total homogenate; *P1*, consisting primarily of unbroken cells and nuclei; *P2*, plasma membrane and larger organelles; *P3*, membranes of smaller organelles; *S3*, cytosol; *LP1*, pellet after hypotonic lysis of synaptosomes and contains larger organelles within synaptosomes; *LP2*, high-spin pellet of LS1 supernatant and containing microsomal fraction within synaptosomes; *LS2*, supernatant of LP2 spin. MW standards are shown on the *left*. *B*, Thrombin digestion of $STEP_{61}$-fusion protein. The released recombinant STEP polypeptide (*lane 1*) was compared with the mobilities of endogenous STEP proteins enriched in P3 fraction (*lane 2*). *C*, N-glycosidase F treatment of P3 membranes. Samples were processed at 37°C overnight in the presence (+) or absence (−) of enzyme. Blots were processed with antibodies against STEP (*top*) or against the control synaptophysin (*p38*, *bottom*). *D*, Distribution of $STEP_{61}$ after sucrose density gradient fractionation and comparison with ER and non-ER-associated proteins. Membrane fractions enriched for the higher MW STEP-immunoreactive peptides (*P3* and *LP2*) were applied to continuous sucrose gradients (0.4–2 M). After ultracentrifugation, equal volumes from each of 12 aliquots were loaded onto 10% SDS polyacrylamide gels and processed in parallel with antibodies against calnexin, STEP, and synaptophysin (*p38*), as indicated on the *right*. MW markers are shown on the *left*.

N-glycosidase F resulted in a faster electrophoretic mobility of synaptophysin (p38), whereas none of the STEP-immunoreactive bands had altered mobilities. These results indicate that the multiple higher MW STEP-immunoreactive bands do not correspond to different N-glycosylated forms of a single STEP polypeptide.

Because $STEP_{61}$ immunoreactivity is enriched in P3 and LP2 fractions, these fractions were processed further through continuous sucrose density gradients. The pattern of STEP immunoreactivity was compared with that of calnexin and synaptophysin in Figure 3*D*. Calnexin is a resident protein of the ER (Wada et al., 1991), whereas synaptophysin is an intrinsic membrane protein of synaptic vesicles (Jahn et al., 1985). In LP2, the peak of STEP-immunoreactivity for the higher MW STEP isoforms colocalized with the peak of calnexin immunoreactivity (fraction 7; 1.04 M sucrose) but not with the peak of synaptophysin (fractions 3–4; 0.61–0.69 M sucrose). In P3 fractions, the peak of STEP-immunoreactivity also overlapped with the peak of calnexin (fraction 9; 1.35 M sucrose), although a second less intense STEP-immunoreactivity peak was detected in fraction 3 (0.60 M sucrose). These results suggest that the higher MW STEP isoforms are enriched in the ER.

The primary amino acid sequence of $STEP_{61}$ predicts for an intrinsic membrane protein with two transmembrane spanning domains. Consistent with that sequence, the higher MW STEP-immunoreactive bands were efficiently released from particulate

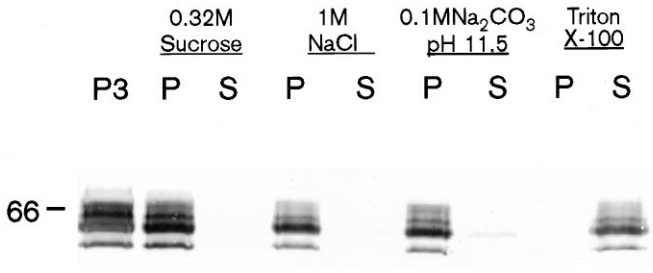

Figure 4. $STEP_{61}$ is an integral membrane protein. Membrane fractions (*P3*) were washed in different buffer conditions as indicated and spun, and pellets (*P*) and supernatants (*S*) were collected. Protein (~50 μg) from each fraction was subjected to SDS-PAGE, transferred to nitrocellulose, and probed with the monoclonal antibody 23E5. The majority of STEP isoforms remain membrane-associated until washed in 2% Triton X-100.

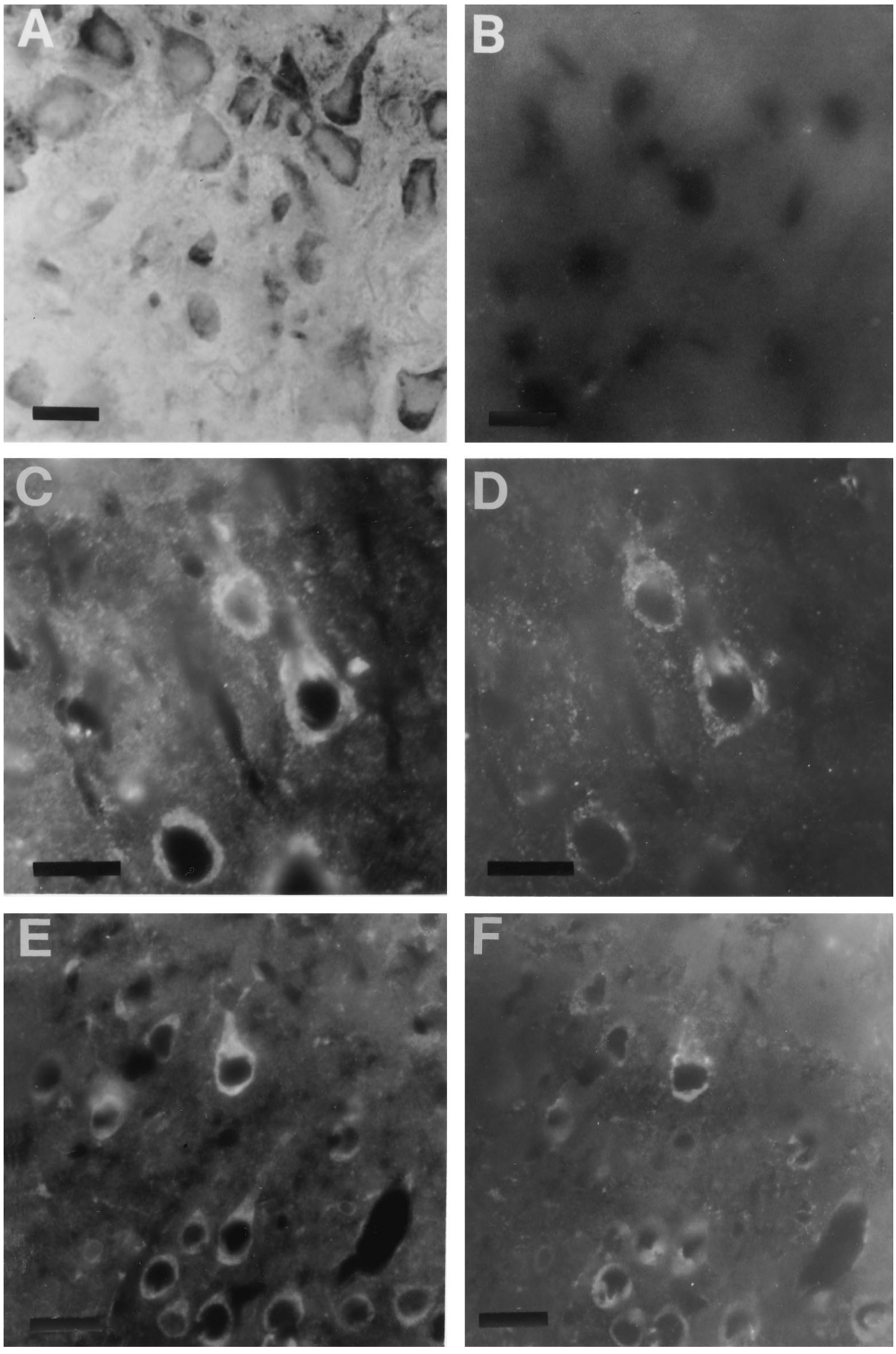

Figure 5. $STEP_{61}$ immunoreactivity is localized in the perinuclear region. *A*, Immunoperoxidase labeling of cortical neurons with Nod antisera showed that the perinuclear region of pyramidal neurons was labeled. *B*, Preabsorption of Nod antisera with $STEP_{61}$ fusion protein eliminated all immunofluorescent staining in control sections. *C–F*, To determine whether STEP immunoreactivity was associated with the ER, immunofluorescent double-labeling studies were performed with the Nod antisera (*C*, *E*) and an antibody specific for PDI, a resident protein of the ER (*D*, *F*). In cortical neurons (*C*, *D*), STEP colocalized with PDI in proximal dendrites and surrounding the nucleus. A similar pattern was also seen in hippocampal neurons (*E*, *F*). Scale bar, 10 μm.

fractions only after washes with detergents, including 2% Triton X-100 (Fig. 4, *lanes 6*, *7*) and SDS (data not shown).

Immunocytochemical analyses

Peroxidase staining or two-color immunofluorescent double labeling was carried out to compare the subcellular distribution of $STEP_{61}$ with PDI, a resident protein of the ER, that acts as a catalyst for rearrangement of disulfide bonds (Vaux et al., 1990). Figure 5*A* shows punctate immunoperoxidase staining of $STEP_{61}$ in pyramidal neurons in the cerebral cortex. The staining in the perinuclear region extended into proximal dendrites. Immunofluorescent double labeling is shown in the remaining panels of Figure 5. Pyramidal neurons of the cerebral cortex contained both $STEP_{61}$ (*C*) and PDI (*D*) immunoreactivity in the perinuclear region. Similarly, in pyramidal neurons of the hippocampus (Fig. 5*E*,*F*), these two markers colocalized in the perinuclear region. PDI immunoreactivity did not extend far into dendrites or axons. Additionally, in the striatum, most neurons exhibited colocalization of both markers in the perinuclear

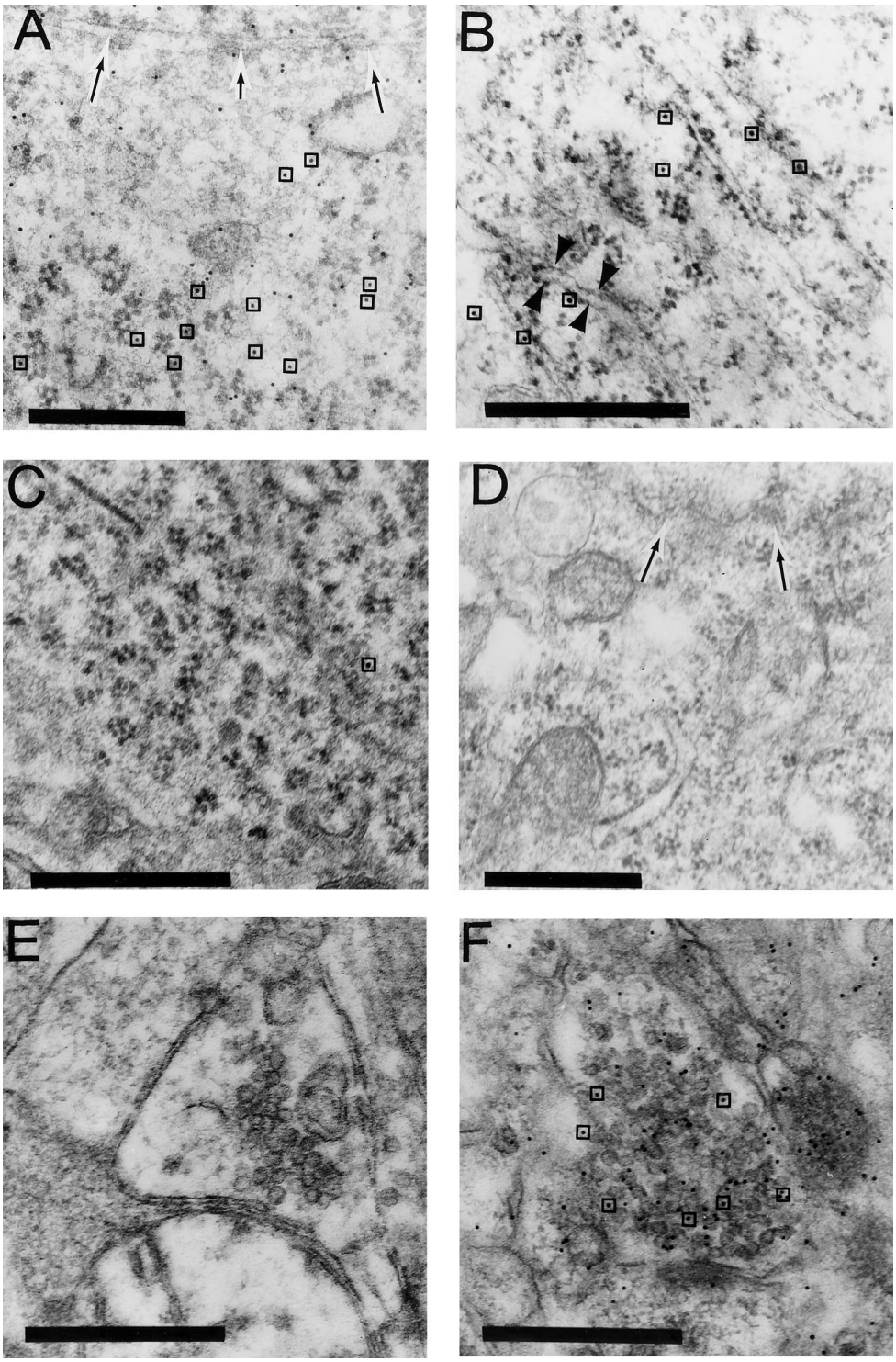

Figure 6. Electron microscopy demonstrates localization of $STEP_{61}$ to ER. In sections incubated in Nod antibody against $STEP_{61}$, a high density of gold particles was evident over free ribosomes (*A*) and the rough ER (*B*). Preabsorption of STEP antisera with STEP peptide-abolished staining (*C*). Specificity of staining was also shown by labeling sections with synaptophysin antibodies, which failed to label rough ER (*D*) but gave strong labeling of synaptic vesicles in terminal boutons (*F*). By contrast, STEP immunogold staining was not observed over more distal processes, including axons and synaptic boutons (*E*). In *A* and *D*, *arrows* indicate nuclear envelope. In *A* and *C*, *boxes* highlight some gold particles to distinguish them from ribosomes. In *B*, *arrowheads* show labeled rough ER. Scale bar, 0.5 μm.

region (data not shown). In contrast to the punctate perinuclear labeling by $STEP_{61}$ antisera, a more diffuse pattern of staining was observed with either monoclonal or polyclonal antisera that recognized both cytosolic and membrane-associated forms of STEP (Lombroso et al., 1993; Boulanger et al., 1995). In control sections, STEP immunostaining was abolished by preabsorbing antiserum with $STEP_{61}$ fusion protein (Fig. 5*B*).

The perinuclear staining for STEP isoforms was confirmed at the ultrastructural level with postembedding immunogold labeling. In the perinuclear region, punctate gold labeling was observed over free ribosomes (Fig. 6*A*) and rough ER (*B*). In control sections, immunogold labeling was abolished by preabsorption of antiserum with $STEP_{61}$ peptide (*C*) or by omission of primary antibodies (data not shown). The Nod antiserum also failed to stain distal processes of neurons, including synaptic boutons (*E*). The specificity of the staining was verified by comparing STEP labeling with that of an antibody against synaptophysin (Fig. 6*D*,*F*). In contrast to the STEP antiserum, synaptophysin antiserum gave little or no background labeling of rough ER in the perinuclear region (*D*), whereas synaptic terminals were

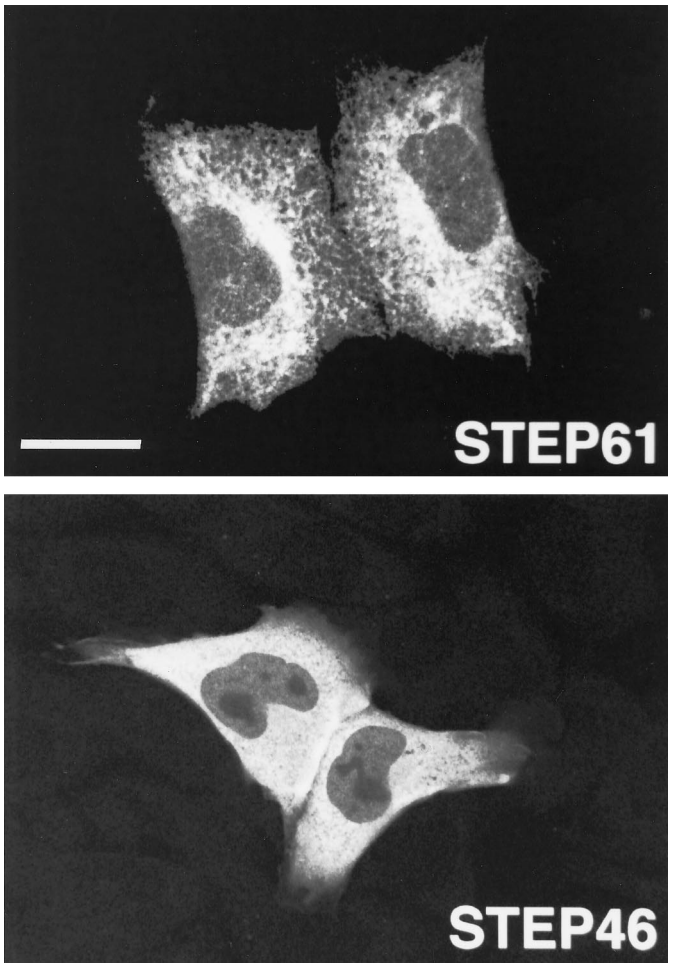

Figure 7. Transfection of $STEP_{61}$ into fibroblasts shows a reticular staining pattern relative to the cytosolic $STEP_{46}$ variant. $STEP_{61}$ and $STEP_{46}$ cDNAs were transiently transfected into CHO cells and detected by immunohistochemistry using the monoclonal antibody 23E5 followed by rhodamine-conjugated goat anti-mouse IgG. In transfected cells, $STEP_{61}$ presented the characteristic reticular distribution of proteins associated with the ER (*top*). Note the perinuclear accumulation of $STEP_{61}$. In contrast, $STEP_{46}$ immunoreactivity was evenly distributed in the cytoplasm of transfected cells, consistent with $STEP_{46}$ being a soluble cytosolic protein (*bottom*). Scale bar, 22 μm.

heavily labeled (*F*). Omission of synaptophysin antibody in the incubation steps eliminated immunogold labeling of synaptic terminals (data not shown).

Transfection experiments

The immunohistochemical and electron microscopic experiments presented above demonstrate that members of the STEP family are present in the ER. An independent line of investigation supports these findings. The full ORFs for $STEP_{61}$ and the cytosolic variant $STEP_{46}$ were transiently transfected into CHO cells, a fibroblast cell line that does not normally express STEP gene products. STEP proteins were localized using immunocytochemical staining with the monoclonal antibody 23E5, which recognizes both STEP isoforms. A reticular pattern of staining was seen after $STEP_{61}$ transfection (Fig. 7, *top*). $STEP_{46}$, instead, was evenly distributed in the cytoplasm, as expected for a soluble cytosolic protein (*bottom*). The polyclonal antibody Nod, generated to recognize membrane and not cytosolic variants, produced a similar staining pattern in

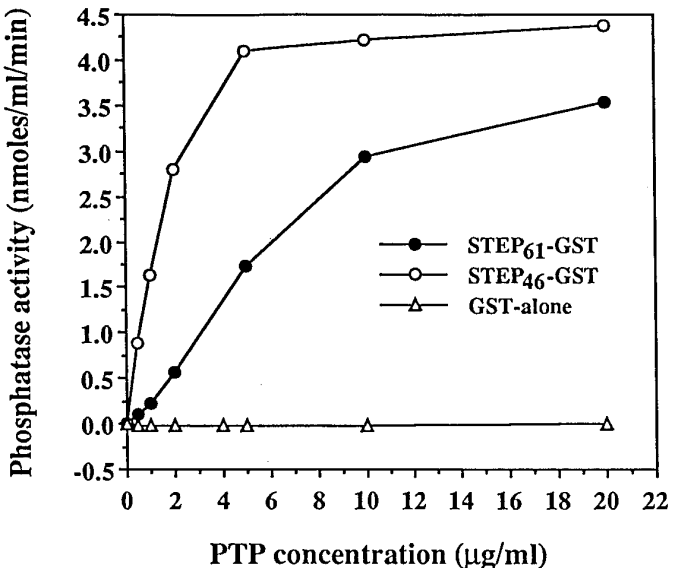

Figure 8. $STEP_{61}$ is less active than the cytosolic variant $STEP_{46}$. The phosphatase activity of the recombinant proteins $STEP_{61}$ and $STEP_{46}$ was compared. $STEP_{61}$ had approximately sixfold less phosphatase activity than $STEP_{46}$. $STEP_{61}$-GST and $STEP_{46}$-GST fusion proteins were affinity-purified on glutathione–agarose beads after induction by IPTG and assayed for phosphatase activity in the presence of 1% Triton-X 100 using the substrate *p*NPP. The values of $STEP_{61}$ and $STEP_{46}$ represent the mean ± SE of two separate assays. GST fusion protein alone (*GST-alone*) is the negative control.

$STEP_{61}$-transfected cells but, as expected, did not stain $STEP_{46}$-transfected cells (data not shown).

Tyrosine phosphatase activity

The phosphatase activity of $STEP_{61}$ was compared with the activity of the cytosolic variant $STEP_{46}$. Because it was possible that the $STEP_{61}$ recombinant protein might form protein aggregates through its two hydrophobic domains, all phosphatase assays were performed in the presence of Triton X-100. $STEP_{61}$-GST fusion protein showed phosphatase activity against *p*NPP substrate, but the level of activity was approximately sixfold lower than that of $STEP_{46}$-GST fusion protein (Fig. 8). Phosphatase assays were also repeated after thrombin cleavage and affinity purification of STEP polypeptides, and $STEP_{61}$ again had approximately 10-fold less activity than $STEP_{46}$. The decrease in $STEP_{61}$ activity thus was not likely to be attributable to the interference of GST. As expected, GST fusion protein alone did not have phosphatase activity.

Both $STEP_{61}$-GST and $STEP_{46}$-GST were inhibited by the tyrosine phosphatase inhibitors sodium vanadate and ammonium molybdate (data not shown). The IC_{50} values for sodium vanadate were 200 nM for $STEP_{61}$-GST and 1 mM for $STEP_{46}$-GST. The IC_{50} values for ammonium molybdate were 400 nM for $STEP_{61}$-GST and 200 nM for $STEP_{46}$-GST. These values are similar to those obtained previously for $STEP_{46}$ (Lombroso et al., 1993).

DISCUSSION

A key point emerging from the present study is that the intracellular distribution of $STEP_{61}$ is markedly different from previously characterized STEP family members. The distinctive localization of $STEP_{61}$ to membrane compartments has been shown by several types of experiments. Taken together, the subcellular fractionations, detergent extractions, and sucrose density gradients clearly

indicate that $STEP_{61}$ is an integral membrane protein and is enriched in fractions in which the endoplasmic reticular protein calnexin is also enriched. Immunofluorescent double labeling for PDI and $STEP_{61}$, as well as electron microscopic localization, demonstrates that $STEP_{61}$ is most enriched in the perinuclear ER. This is in contrast to the more diffuse pattern of neuronal staining that was seen with antibodies generated to recognize all STEP isoforms (Lombroso et al., 1993; Boulanger et al., 1995), suggesting that the polyclonal antibody (Nod) recognizes a subgroup of STEP isoforms.

The transfection experiments provide additional support for these findings. In isolation, transfection experiments must be viewed with caution, because it is known that some proteins are not targeted to their proper final destination when transfected into cells that do not normally process them. However, the purpose of these experiments was to determine the targeting pattern of recombinant $STEP_{61}$ in cells that do not have additional STEP isoforms present and compare it to the pattern seen with the cytosolic variant $STEP_{46}$. The results lend support to the hypothesis that the N-terminal region of $STEP_{61}$ confers to this protein an intracellular localization pattern that is distinct from the cytosolic pattern seen with $STEP_{46}$.

Although these experiments do not rule out the possibility that a pool of $STEP_{61}$ is associated with other membrane compartments, they clearly show that $STEP_{61}$ is enriched in the ER of neurons. The presence of two hydrophobic domains in $STEP_{61}$ that are not present in other known STEP variants suggests that these domains provide the necessary information for the selective compartmentalization of $STEP_{61}$ to neuronal ER. The differential centrifugation results indicate that several other higher MW membrane-associated STEP isoforms exist, as well as a pool of lower MW STEP protein that are present in both particulate and soluble fractions (Fig. 3*A*). It is possible that these STEP isoforms will also be found to localize to the ER or to additional intracellular membranes. However, the antiserum used in this study failed to detect SDS-denatured proteins on Western blots and could not be used to test this hypothesis. To identify the subcellular targets of these other variants, specific antibodies will need to be generated.

The present study supports recent findings of important amino acid domains outside the phosphatase domain. For example, PTPs have been identified containing *Src* homology 2 domains (Shen et al., 1991; Matthews et al., 1992; Plutzky et al., 1992; Yi et al., 1992; Pawson, 1995), and polyproline-rich sequences that match the consensus sequence for the binding site of *Src* homology 3 domains have also been identified (Sawada et al., 1994). These domains are thought to provide a mechanism by which PTPs associate with downstream effector molecules.

A number of studies have demonstrated that alternative splicing is responsible for targeting PTPs to distinct intracellular regions and compartments (Matthews et al., 1990; Price, 1992; McLaughlin and Dixon, 1993; Oon et al., 1993; Mauro and Dixon, 1994; Elson and Leder, 1995). This has the effect of compartmentalizing PTPs in the vicinity of their substrates or anchoring them to membrane storage sites until released or activated by appropriate intracellular signals. The present study on $STEP_{61}$ extends these findings to the CNS. We have shown that alternative splicing within the STEP family leads to the production of either cytosolic polypeptides or proteins targeted to the ER.

Although the functional significance of having $STEP_{61}$ associated with the ER is not yet known, recent studies on a sterol regulatory element-binding protein 1 (SREBP-1) are relevant. SREBP-1 is a transcription factor that is synthesized as a 125 kDa precursor attached to the nuclear envelope and ER (Wang et al., 1994). Under the appropriate cellular signal (low intracellular concentration of cholesterol), the membrane-bound precursor is cleaved to generate a smaller cytosolic fragment that rapidly translocates to the nucleus, where it activates transcription of proteins involved in sterol pathways (Wang et al., 1994).

Several observations suggest that an analogous mechanism might be at work with $STEP_{61}$. We have shown that $STEP_{61}$ is bound to the ER membrane. In addition, PEST sequences are present, and these sequences are thought to signal proteolytic cleavage of the proteins in which they are found. They have now been identified in several additional PTPs (Matthews et al., 1992; Takekawa et al., 1992; Yang et al., 1993; Garton and Tonks, 1994), although it has not yet been determined in these proteins whether the PEST sequences are functional. If proteolysis of $STEP_{61}$ were to occur, then the predicted MW of the largest released fragment would be ~44 kDa. This size is close to the observed mobilities of some members of the cytosolic group of STEP-immunoreactive proteins. In future studies, it may be possible to determine whether higher MW STEP proteins are cleaved to release the cytosolic isoforms by employing [^{35}S]methionine pulse chase experiments. Alternatively, careful peptide mapping or amino acid sequencing of each of the STEP immunoreactive bands will be necessary to determine the relationship of the different variants to each other.

Similarly to STEP, two other intracellular PTPs that have been localized to the ER (Frangioni et al., 1993; Lorenzen et al., 1995). It is interesting to note that proteolysis has been suggested as a mechanism that modulates the enzymatic activity for both of these PTPs. Cleavage of the C-terminal sequence of T-cell PTP stimulates its phosphatase activity *in vitro* (Cool et al., 1990; Zander et al., 1991), and PTP1B shows a twofold increase of phosphatase activity after limited proteolysis by calpain (Frangioni et al., 1993).

In this study, we have shown that the recombinant membrane-associated isoform $STEP_{61}$ has significantly less phosphatase activity than the cytosolic variant $STEP_{46}$. This was a surprising observation, because $STEP_{46}$ is contained entirely within $STEP_{61}$, and the only difference in their sequences are the novel 172 amino acids at the N terminus of $STEP_{61}$. There are several possible explanations for the observed decrease in enzymatic activity. The N-terminal extension of the recombinant $STEP_{61}$ protein may directly interfere by limiting the accessibility of *p*NPP to the catalytic domain. In addition, aggregation of recombinant protein is likely to occur through the two hydrophobic domains. We attempted to address these issues by performing all enzymatic assays in the presence of detergent as well as digesting with thrombin before phosphatase assays. The difference in activity remained, suggesting that neither protein aggregation nor interference by GST accounts for the decrease of phosphatase activity seen with $STEP_{61}$. Nonetheless, the assays were conducted against an artificial substrate, and additional work is required to demonstrate whether this decrease in activity occurs *in vivo*.

In addition to the PEST sequences, $STEP_{61}$ has two polyproline motifs that match the consensus sequence for the binding site of SH3 domains (Ren et al., 1993; Cohen et al., 1995). Each of the PEST sequences contains one of the polyproline-rich domains and suggests a possible functional relationship. Protein–protein interactions are capable of masking underlying PEST signals, thereby preventing proteolysis of these proteins and prolonging their half-life (Shanklin et al., 1987; Rechsteiner, 1988).

Based on these considerations, a model for how $STEP_{61}$ func-

tions within neurons can now be proposed. $STEP_{61}$ is normally attached to membrane compartments. In this form, $STEP_{61}$ interacts with other protein(s), and these protein–protein interactions mask underlying PEST sequences. Only after neuronal stimulation (e.g., growth factor or neurotransmitter binding that leads to phosphorylation or Ca^{2+} influx) are the protein–protein complexes disrupted and the proteolytic sites exposed. $STEP_{61}$ is then cleaved, and smaller isoforms are released into the cytosol.

In conclusion, the present study has characterized a new member of the STEP family of brain-enriched PTPs. We have shown that this family consists of cytosolic and transmembrane isoforms produced by alternative splicing mechanisms. The biological effects of alternative splicing include changing the subcellular localization of protein isoforms as well as modulating their enzymatic activity. The significance of these mechanisms is especially evident when the proteins are regulatory molecules, such as PTPs, in which subtle changes in their structure may effect their localization pattern, enzymatic activity, or potential access to substrate molecules.

REFERENCES

Atashi JR, Klinz SG, Ingraham CA, Matten WT, Schachner M, Maness PF (1992) Neural cell adhesion molecules modulate tyrosine phosphorylation of tubulin in nerve growth cone membranes. Neuron 8:831–842.

Boulanger LM, Lombroso PJ, Raghunathan A, During MJ, Wahle P, Naegele JR (1995) Cellular and molecular characterization of a brain-enriched protein tyrosine phosphatase. J Neurosci 15:1532–1544.

Bradford MM (1976) A rapid and sensitive method for the quantification of microgram quantities of protein utilizing the principle of protein-dye binding. Anal Biochem 72:248–254.

Bult A, Naegele JR, Sharma E, Lombroso PJ (1995) Isolation and characterization of brain enriched protein tyrosine phosphatases. Neuroprotocols 6:91–104.

Cameron PL, Südhof TC, Jahn R, De Camilli P (1991) Colocalization of synaptophysin with transferrin receptors: implications for synaptic vesicle biogenesis. J Cell Biol 115:151–164.

Charbonneau H, Tonks NK (1992) 1002 protein phosphatases? Annu Rev Cell Biol 8:463–493.

Charbonneau H, Tonks NK, Dumar S, Diltz C, Harrylock M, Cool DE, Krebs EG, Fischer EJ, Walsh KA (1989) Human placenta protein-tyrosine-phosphatase: amino acid sequence and relationship to a family of receptor-like proteins. Proc Natl Acad Sci USA 89:5252–5256.

Cohen GB, Ren R, Baltimore D (1995) Modular binding domains in signal transduction proteins. Cell 80:237–248.

Cool D, Tonks N, Charbonneau H, Walsh K, Fischer E, Krebs E (1990) Expression of a human T-cell protein-tyrosine-phosphatase in baby hamster kidney cells. Proc Natl Acad Sci USA 87:7280–7284.

Cordon-Cardo C, Tapley P, Jing S, Nanduri V, O'Rourke E, Lamballe F, Kovary K, Klein R, Jones KR, Reichardt LF, Barbacid M (1991) The trk tyrosine protein kinase mediates the mitogenic properties of nerve growth factor and neurotrophin-3. Cell 66:1–20.

Cudmore SB, Gurd JW (1991) Postnatal age and protein tyrosine phosphorylation at synapses in the developing rat brain. J Neurochem 57:1240–1248.

Desai C, Gindhart J, Goldstein L, Zinn K (1996) Receptor tyrosine phosphatases are required for motor axon guidance in the *Drosophila* embryo. Cell 84:599–609.

Doherty P, Walsh FS (1992) Cell adhesion molecules, second messengers and axonal growth. Curr Opin Neurobiol 2:595–601.

Dunn JA, Kirsch JD, Naegele JR (1995) Transient immunoglobulin-like molecules are present in the subplate zone and cerebral cortex during postnatal development. Cereb Cortex 5:494–505.

Elson A, Leder P (1995) Identification of a cytoplasmic, phorbol ester-inducible isoform of protein tyrosine phosphatase epsilon. Cell Biol 92:12235–12239.

Faure R, Posner B (1993) Differential intracellular compartmentalization of phosphotyrosine phosphatases in a glial cell line: TC-PTP versus PTP-1B. Glia 9:311–314.

Fischer EH, Charbonneau H, Tonks NK (1991) Protein tyrosine phosphatases: a diverse family of intracellular and transmembrane enzymes. Science 253:401–406.

Flores E, Roy G, Patel D, Shaw A, Thomas M (1994) Nuclear localization of the PEP protein tyrosine phosphatase. Mol Cell Bio 14:4938–4946.

Frangioni JV, Beahm PH, Shifrin V, Jost CA, Neel BG (1992) The nontransmembrane tyrosine phosphatase PTP1B localizes to the endoplasmic reticulum via its 35 amino acid C-terminal sequence. Cell 68:545–560.

Frangioni JV, Oda A, Smith M, Salzman EW, Neel BG (1993) Calpain-catalyzed cleavage and subcellular relocation of protein phosphotyrosine phosphatase 1B (PTP-1B) in human platelets. EMBO J 12:4843–4856.

Fujiki Y, Hubard A, Fowler S, Lazarow P (1982) Isolation of intracellular membranes by means of sodium carbonate treatment: application to endoplasmic reticulum. J Cell Biol 93:97–102.

Garton A, Tonks N (1994) PTP-PEST: a protein tyrosine phosphatase regulated by serine phosphorylation. EMBO J 13:3763–71.

Girault J-A, Chamak B, Bertuzzi G, Tixier H, Wang JK, Pang DT, Greengard P (1992) Protein phosphotyrosine in mouse brain: developmental changes and regulation by epidermal growth factor, type I insulin-like growth factor, and insulin. J Neurochem 58:518–528.

Griffiths G, McDowall A, Back R, Dubocher J (1984) On the preparation of cryosections for immunocytochemistry. J Ultrastruct Res 89:65–78.

Gu MX, York JD, Warshawsky I, Majerus PW (1991) Identification, cloning, and expression of a cytosolic megakaryocyte protein-tyrosine-phosphatase with sequence homology to cytoskeletal protein 4.1. Proc Natl Acad Sci USA 88:5867–5871.

Huttner WB, Schiebler W, Greengard P, DeCamilli P (1983) Synapsin I (protein I), a nerve terminal specific phosphoprotein. III. Its association with synaptic vesicles studied in a highly purified synaptic vesicle preparation. J Cell Biol 96:1374–1388.

Jahn R, Schiebler W, Ouimet C, Greengard P (1985) A 38,000-dalton membrane protein (p38) present in synaptic vesicles. Proc Natl Acad Sci USA 82:4137–4141.

Kaplan DR, Hempstead BL, Martin-Zanca D, Chao MV, Parada LF (1991) The *trk* proto-oncogene product: a signal transducing receptor for nerve growth factor. Science 252:554–557.

Klein R, Jing S, Nanduri V, O'Rourke E, Barbacid M (1991) The *trk* proto-oncogene encodes a receptor for nerve growth factor. Cell 65:189–197.

Krueger N, Van Vactor D, Wan H, Gelbart W, Goodman C, Saito H (1996) The transmembrane tyrosine phosphatase DLAR controls motor axon guidance in *Drosophila*. Cell 84:611–622.

Laemmli UK (1970) Cleavage of structural proteins during the preassembly of the head of bacteriophage T4. Nature 227:680–685.

Li X, Luna J, Lombroso P, Francke U (1995) Molecular cloning of the human homolog of a striatum-enriched phosphatase (STEP) gene and chromosomal mapping of the human and murine loci. Genomics 28:442–449.

Lombroso PJ, Murdoch G, Lerner M (1991) Molecular characterization of a protein-tyrosine phosphatase enriched in striatum. Proc Natl Acad Sci USA 88:7242–7246.

Lombroso PJ, Naegele JR, Sharma E, Lerner M (1993) A protein tyrosine phosphatase expressed within dopaminoceptive neurons of the basal ganglia and related structures. J Neurosci 13:3064–3074.

Lorenzen JA, Dadabay CY, Fischer EH (1995) COOH-terminal sequence motifs target the T cell protein phosphatase to the ER and nucleus. J Cell Biol 131:631–643.

Maness PF, Aubury M, Shores CG, Frame L, Pfenniger KH (1988) c-src gene product in developing rat brain is enriched in nerve growth cone membranes. Proc Natl Acad Sci USA 85:5001–5005.

Matthews R, Cahir E, Thomas M (1990) Identification of an additional member of the protein tyrosine phosphatase family: evidence for alternative splicing in the PTP domain. Proc Natl Acad Sci USA 87:4444–4448.

Matthews R, Bowne D, Flores E, Thomas M (1992) Characterization of hematopoietic intracellular protein tyrosine phosphatases: description of a phosphatase containing an SH2 domain and another enriched in proline-, glutamic acid-, serine-, and threonine-rich sequences. Mol Cell Biol 12:2396–2405.

Mauro LJ, Dixon JE (1994) "Zip codes" direct intracellular protein tyrosine phosphatases to the correct cellular "address." Trends Biochem Sci 19:151–155.

McLaughlin S, Dixon JE (1993) Alternative splicing gives rise to a nuclear protein tyrosine phosphatase in *Drosophila*. J Biol Chem 268:6839–6842.

Naegele J, Barnstable C (1991) A carbohydrate epitope defined by monoclonal antibody VC1.1 is found on N-CAM and other cell adhesion molecules. Brain Res 559:118–129.

Naegele J, Lombroso P (1994) Protein tyrosine phosphatases in the central nervous system. Crit Rev Neurobiol 9:115–124.

Naegele J, Arimatsu Y, Schwartz P, Barnstable C (1988) Selective staining of a subset of GABAergic neurons in cat visual cortex by monoclonal antibody VC1.1. J Neurosci 8:79–89.

Oon S, Hong A, Yang X, Chia W (1993) Alternative splicing in a novel tyrosine phosphatase gene (DPTP4E) of *Drosophila melanogaster* generates two large receptor-like proteins which differ in their carboxyl termini. J Biol Chem 268:23964–23971.

Pawson T (1995) Protein modules and signalling networks. Nature 373:573–580.

Plutzky J, Neel B, Rosenberg R (1992) Isolation of a src homology 2-containing tyrosine phosphatase. Proc Natl Acad Sci USA 89:1123–1127.

Price BD (1992) Signalling across the endoplasmic reticulum membrane: potential mechanisms. Cell Signal 4:465–470.

Qu Z, Moritz E, Huganir RL (1990) Regulation of tyrosine phosphorylation of the nicotinic acetylcholine receptor at the rat neuromuscular junction. Neuron 2:367–378.

Raghunathan A, Matthews G, Lombroso P, Naegele J (1996) Transient compartmental expression of a family of protein tyrosine phosphatases in the developing striatum. Dev Brain Res 91:190–199.

Rechsteiner M (1988) Regulation of enzyme levels by proteolysis: the role of pest regions. Adv Enzyme Regul 27:135–151.

Rehm H, Wiedenmann B, Betz H (1986) Molecular characterization of synaptophysin, a major calcium-binding protein of the synaptic vesicle membrane. EMBO J 5:535–541.

Ren R, Mayer BJ, Cicchetti P, Baltimore D (1993) Identification of a 10-amino acid proline-rich SH3 binding site. Science 259:1157–1161.

Rogers S, Wells R, M Rechsteiner (1986) Amino acid sequences common to rapidly degraded proteins: the PEST hypothesis. Science 234:364–368.

Sahin M, Hockfield S (1993) Protein tyrosine phosphatases expressed in the developing rat brain. J Neurosci 13:4968–4978.

Sawada M, Ogata M, Fujino Y, Hamaoka T (1994) cDNA cloning of a novel protein tyrosine phosphatase with homology to cytoskeletal protein 4.1 and its expression in T-lineage cells. Biochem Biophys Res Commun 203:479–484.

Schlessinger J, Ullrich A (1992) Growth factor signaling by receptor tyrosine kinases. Neuron 9:383–391.

Shanklin J, Jabben M, Vierstra R (1987) Red light-induced formation of ubiquitin-phytochrome conjugates: identification of possible intermediates of phytochrome degradation. Proc Natl Acad Sci USA 84:359–363.

Sharma E, Zhao F, Bult A, Lombroso PJ (1995) Isolation and characterization of $STEP_{20}$: an isoform of a family of brain-enriched protein tyrosine phosphatases. Mol Brain Res 32:87–93.

Shen S, Bastien L, Posner B, Chretien P (1991) A protein-tyrosine phosphatase with sequence similarity to the SH2 domain of the protein-tyrosine kinases. Nature 352:736–739.

Smith DB, Johnson KS (1988) Single step purification of polypeptides expressed in *E. coli* as fusions with glutathione S-transferase. Gene 67:31–40.

Solimena M, Aggujaro D, Muntzel C, Dirkx R, Butler M, De Camilli P, Hayday A (1993) Association of GAD65, but not of GAD67, with the Golgi complex is mediated by the NH2 terminal region. Proc Natl Acad Sci USA 90:3073–3077.

Solimena M, Dirkx R, Hermel J-M, Pleasic-Williams S, Shapiro JA, Rabin DU (1996) ICA 512, an autoantigen of insulin-dependent diabetes mellitus is an ubiquitous intrinsic membrane protein of neurosecretory granules. EMBO J 15:2102–2114.

Takekawa M, Itoh F, Hinoda Y, Arimura Y, Toyota M, Sekiya M, Adachi M, Imai K, Yachi A (1992) Cloning and characterization of a human cDNA encoding a novel putative cytoplasmic protein-tyrosine-phosphatase. Biochem Biophys Res Commun 189:1223–1230.

Tonks NK, Yang Q, Guida P (1991) Structure, regulation, and function of protein tyrosine phosphatases. Cold Spring Harb Symp Quant Biol 56:265–273.

Towbin H, Staehelin T, Gordon J (1979) Electrophoretic transfer of proteins from polyacrylamide gels to nitrocellulose sheets: procedure and some applications. Proc Natl Acad Sci USA 76:4350–4354.

Vaux D, Tooze J, Fuller S (1990) Identification by anti-idiotype antibodies of an intracellular membrane protein that recognizes a mammalian endoplasmic reticulum retention signal. Nature 345:495–502.

Wada I, Rindress D, Cameron P, Ou W, Doherty J, Louvard D, Bell A, Dignard D, Thomas D, Bergeron J (1991) SSRα and associated calnexin are major calcium binding proteins of the endoplasmic reticulum membrane. J Biol Chem 266:19599–19610.

Walch-Solimena C, Takei K, Marek K, Midyett K, Sudhof T, De Camilli P, Jahn R (1993) Synaptotagmin: a membrane constituent of neuropeptide-containing large dense-core vesicles. J Neurosci 13:3895–3903.

Walton DM, Dixon JE (1993) Protein tyrosine phosphatase. Annu Rev Biochem 62:101–120.

Walton KM, Martell KJ, Kwak SP, Dixon JE, Largent BL (1993) A novel receptor-type protein tyrosine phosphatase is expressed during neurogenesis in the olfactory neuroepithelium. Neuron 11:387–400.

Wang K, Villalobo A, Roufogalis B (1989) Calmodulin-binding proteins as calpain substrates. Biochem J 262:693–706.

Wang X, Sato R, Brown M, Hua X, Goldstein J (1994) SREBP-1, a membrane-bound transcription factor released by sterol-regulated proteolysis. Cell 77:53–62.

Winslow J, Moran P, Valverde J, Shih A, Yuan J, Wong S, Tsai S, Goddard A, Henzel W, Hefti F, Beck K, Caras I (1995) Cloning of AL-1, a ligand for an Eph-related tyrosine kinase receptor involved in axon bundle formation. Neuron 14:973–981.

Woodford-Thomas TA, Rhodes JD, Dixon JE (1992) Expression of a protein tyrosine phosphatase in normal and *v-src*-transformed mouse 3T3 fibroblasts. J Cell Biol 117:401–414.

Yang Q, Tonks NK (1991) Isolation of a cDNA clone encoding a human protein-tyrosine phosphatase with homology to the cytoskeletal-associated proteins band 4.1, ezrin, and talin. Proc Natl Acad Sci USA 88:5949–5953.

Yang Q, Co D, Sommercorn J, Tonks NK (1993) Cloning and expression of PTP-PEST. A novel, human, nontransmembrane protein tyrosine phosphatase. J Biol Chem 268:6622–6628.

Yi T, Cleveland J, Ihle J (1992) Protein tyrosine phosphatase containing SH2 domains: characterization, preferential expression in hematopoietic cells, and localization to human chromosome 12p12–p13. Mol Cell Biol 12:836–846.

Yu H, Chen JK, Feng S, Dalgarno DC, Brauer AW, Schreiber SL (1994) Structural basis for the binding of proline-rich peptides to SH3 domains. Cell 76:933–945.

Zander NF, Lorenzen J, Cool D, Tonks N, Daum G, Krebs E, Fischer E (1991) Purification and characterization of a human recombinant T-cell protein-tyrosine-phosphatase from a baculovirus expression system. Biochemistry 30:6964–6970.

Zhang JS, Longo FM (1995) LAR tyrosine phosphatase receptor: alternative splicing is preferential to the nervous system, coordinated with cell growth and generates novel isoforms containing extensive CAG repeats. J Cell Biol 128:415–431.